THE ASTROPHYSICAL JOURNAL, 406:142–157, 1993 March 20

THE LOW-MASS STELLAR CONTENT OF GALAXIES: CONSTRAINTS THROUGH HYBRID POPULATION SYNTHESIS NEAR 1 MICRON

JEAN COUTURE[1] AND EDUARDO HARDY[2,3]

Received 1992 May 17; accepted 1992 September 24

ABSTRACT

We present high signal-to-noise observations obtained with the RC spectrograph at the CTIO 4 m telescope of six galaxies and of a variety of dwarfs and galactic bulge giants in the 9800–10200 Å spectral range. This spectral region contains gravity-sensitive bands of the FeH molecule. The Wing-Ford band of FeH centered at 9916 Å is clearly identified in all galaxies. A variety of modeling procedures employing the stellar library are used to reproduce the observed galactic spectra over this spectral range, and a method is described of scanning the solution space in search of secondary minima in the optimized synthesis procedure. We assume a power-law representation of the mass function with a slope "x" and a lower cutoff mass m_{low}. In order to test for these parameters we introduce a hybrid synthesis method which combines a sub-library of evolutionary-derived populations of known parameters, with a sub-library composed of individual late giants in advanced evolutionary phases. Although strong constraints for the "x" and m_{low} parameters are not obtained within our limited spectral interval, a valid range of parameters is isolated. On the other hand, no combination of model parameters is capable of producing a luminosity contribution of M dwarfs in the I band larger than 10%–20%. The total luminosity contribution in the I band coming from all dwarfs would rarely exceed 30%–40%. Populations with a Salpeter exponent of the mass function will contribute on average less than 5% of the light in the I band from M dwarfs and less than 20% from all dwarfs.

Subject headings: galaxies: stellar content — infrared: galaxies — stars: late-type — stars: luminosity function, mass function

1. INTRODUCTION

Studies of the low main sequence in the 0.1–0.2 $M_\odot$ interval in galaxies are essential to set nondynamical constraints on the amount of mass stored in faint dwarfs and to derive information on the shape of the initial mass function (IMF). Because the integrated light in galaxies is very sensitive at long wavelengths to the contribution of red giants, only strong spectral features could provide the required dwarf/giant discrimination. In the near-IR the CO feature near 2 μm is capable of providing a dilution measure of the presence of late M dwarfs (i.e., Davidge 1990a, b). Towards shorter wavelengths the range between 8000 Å and 1 μm is a particularly useful spectral interval because it contains three main spectral discriminators of the dwarf/giant ratio. The first two are (1) the infrared Na I doublet (IR Na I) with components at 8183 and 8195 Å which is sensitive to the presence of late dwarfs (Cohen 1978; Faber & French 1980), and (2) the infrared Ca II triplet at 8498, 8542, and 8662 Å (Jones, Alloin, & Jones 1984) which is sensitive to the presence of giants. Extensive measurements of these first two features have been performed recently by Delisle & Hardy (1992) who discuss their dependence on metallicity. They found, by measurements at the center of galaxies, that the strength of the Na indices correlates both with the strength of the Mg_2 metallicity indicator and with the absolute magnitude of the Galaxy. It was concluded that the evidence claimed (i.e., Faber & French 1980; Boroson & Thompson 1991) for dwarf enrichment of the central regions of early type galaxies on the basis of the Na feature, as measured by spectral indices, was very likely the result of metallicity effects. Delisle & Hardy's (1992) conclusion was reinforced by their study of spectral gradients in both features.

It would seem that the best hope of detecting the contribution of late M dwarfs is provided by the third feature, the Wing-Ford band (hereafter WFB), corresponding to the (0–0) band of the $^4\Delta$–$^4\Delta$ system of the iron hydride FeH molecule centered at 9916 Å and with band head at 9896 Å, which is remarkably strong in late M dwarfs. The first spectroscopic detections of this feature in the integrated spectra of elliptical galaxies were obtained by Hardy & Couture (1988, hereafter Paper I), and Hardy (1990). The study of the Wing-Ford band in galaxies was pioneered by Whitford (1977) who measured its strength by using fixed narrow IDS bandpasses located at continuum and line positions. It should be pointed out that this feature is but the most prominent of a series of bands of the FeH molecule covering the 9880–10070 Å spectral interval (i.e., Kirkpatrick et al. 1993; Phillips et al. 1987).

The present paper readdresses the problem of the low-mass stellar content of galaxies, posed in Paper I, with the help of new galaxy and stellar data and new analytical techniques. We try to answer the following questions. Are our new measurements of the WFB indices compatible with the results of Whitford's (1977), and are our models compatible with his? What are the mass functions that best describe the galaxy spectra, and are they the same from galaxy to galaxy? What is the maximum percentage of near-IR light coming from late main-sequence stars that is allowed by the models?

This paper is organized as follows. In § 2 we will briefly discuss the observations and the data reduction procedures; in § 3 we present and discuss measurements of *indices* that characterize the WFB. We then examine in § 4 the stellar content of

[1] Department of Physics and Astronomy, McMaster University, Hamilton, Ontario, Canada L8S 4M1.
[2] Département de Physique, Université Laval, and Observatoire du mont Mégantic, Sainte-Foy, Québec, Canada G1K 7P4.
[3] Visiting Observer, Cerro Tololo Inter-American Observatory, operated by Associated Universities for Research in Astronomy, Inc., under contract with the National Science Foundation.

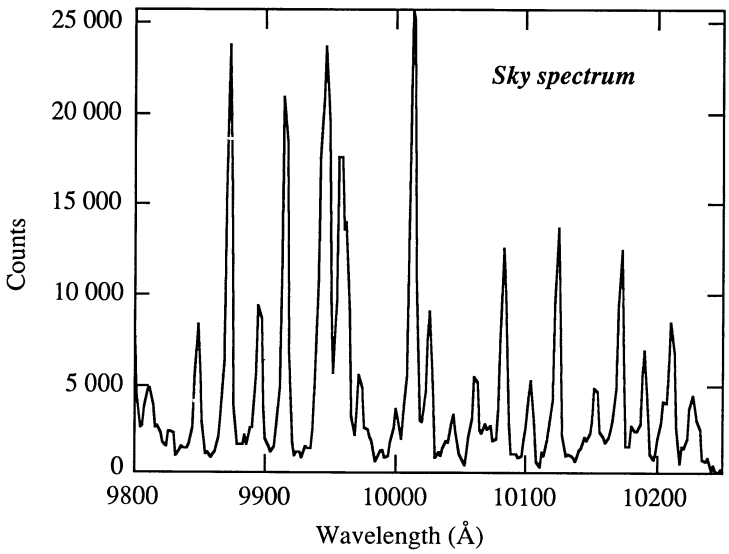

FIG. 1.—A 10 minute exposure of a 4″ × 2″ sky section near NGC 3379 showing the strong Meinel OH bands. The top of the emission centered at 10013 Å corresponds to 20% of the signal at this wavelength at the center of the galaxy.

the present sample of ellipticals and bulges by applying our optimization spectral synthesis package (see Couture & Hardy 1990) with the help of the stellar data in our spectral library. We will finally build, in § 5, a set of evolutionary stellar populations which will then be used in our new hybrid population synthesis method (hereafter HPS). The aim will be to quantify the physical parameters characterizing the galaxy spectra within the full wavelength region observed, and to set limits to the light contribution coming from late dwarfs. A summary and a brief discussion of the results obtained and the limitations of the methods employed are presented in § 6.

2. OBSERVATIONS AND DATA REDUCTION

All spectroscopic observations used in this paper were obtained at CTIO. The galaxy data base comprises a total of six ellipticals and spheroids listed in Table 1. Concurrently, a number of stars of different spectral types and metallicities, including metal-rich giants in the galactic bulge, were observed in order to build a spectral library for synthesis purposes. These stars are listed in columns (1) and (7) of Table 2. The data were obtained at the 4 m telescope with a spectral resolution of 4 Å FWHM in the 9500–10300 Å interval using the Air Schmidt camera, and a GEC CCD detector. Galactic and stellar spectra achieved signal-to-noise ratios of at least 100 per Å after sky subtraction.

The main technical problems encountered in this type of observations are in order of importance: (a) the strong contamination arising from the bright night-sky OH Meinel emission bands shown in Figure 1, which must be very carefully subtracted as their peaks contribute ~20% of the total signal at their wavelengths near the centers of bright galaxies. (b) Water vapor absorption must be accounted for by concurrent observations of early-type stars. (c) Because of the weakness of the FeH feature near 1 μm (~1.5% of the continuum) special care must be taken in flat-fielding the data. As discussed in Paper I the comparison spectrum of each galaxy exposure was used to assign precise wavelengths to the sky lines contained in that galaxy frame. These lines were then used in turn as a new comparison spectrum to transform the frame to a wavelength scale and, together with a multihole frame, to perform a two-dimensional geometrical rectification of each frame prior to the usual background subtraction. This amounted to a form of sky self-subtraction. Terrestrial H_2O vapor turned out not to be a major problem in the 9800–10250 Å region.

Comparison of flux standards observed on each of the three nights indicates that the instrumental system was stable to within the measurable precision. The observations were not fluxed because fluxing in this wavelength interval is imprecise and tends to introduce spectral oscillations. Rather, all observations of galaxies and stars were kept in the instrumental system, but were divided by a smooth common sensitivity curve that approximates well a standard continuum for the galaxies. All spectra were then normalized through division by the average value of the intensity within a small bandpass centered around 10100 Å. The spectral resolution of 4 Å FWHM corresponds to a velocity Gaussian sigma of ~50 km s^{-1}, much smaller than the central velocity dispersions of the galaxies listed in column (4) of Table 1. The galaxy observations are therefore limited in resolution by the intrinsic central velocity dispersion, whereas the stellar observations are limited by the instrumental resolution. Consequently, we have convolved the stellar spectra with an appropriate Gaussian so as to render both the stellar and the galaxy libraries comparable and thus avoid the possible effects of spectral mismatching.

We show in Figure 2 the WFB feature for late M dwarfs. This figure makes evident the steep dependence of the FeH strength with spectral type for these stars. Late M giants are shown for comparison in Figure 3 where it can be seen that the δ system of TiO, of which the (2–3) component overlaps the WFB spectral region, is progressively stronger. The progression of band strengths along the (1–2), (2–3), and (3–4) sequence of the δ system of TiO demonstrated by Lockwood (1973) suggests that the FeH molecule does not contribute appreciably to the strengths of the δ(2–3) band in giants. Among dwarf stars, on the other hand, the δ system of TiO

TABLE 1

WING-FORD BAND MEASUREMENT IN GALAXIES

Galaxies (1)	Type (2)	V_{rad} (km s^{-1}) (3)	σ_V[a] (km s^{-1}) (4)	Δ_1 (mag) (5)	σ (mag) (6)	Δ_2 (mag) (7)
NGC 1617.....	Sa	1040	...	0.011	0.002	0.012
NGC 1672.....	Sb	1335	...	0.003	0.003	0.008
NGC 3379.....	E0	893	218	0.014	0.002	0.016
NGC 4406.....	E3	−250	256	0.017	0.003	0.017
NGC 4472.....	E1	961	315	0.015	0.002	0.021
NGC 4742.....	E4	1221	108	0.017	0.003	0.024

[a] From Whitmore, McElroy, & Tonry 1985.

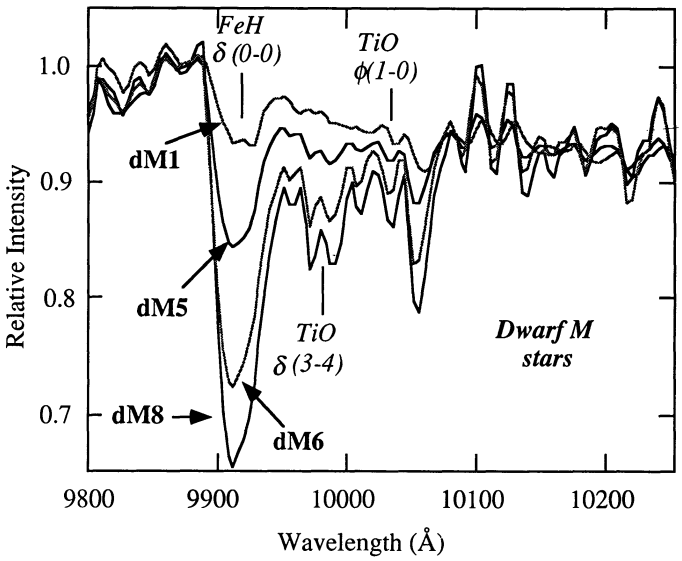

FIG. 2.—Spectral energy distribution of representative M dwarfs showing the strong dependence of the strength of the (0–0) band of the $^4\Delta$–$^4\Delta$ system of the iron hydride FeH molecule with spectral type. The absorption feature near 10050 Å is probably composed of FeH transitions. TiO bands are also shown.

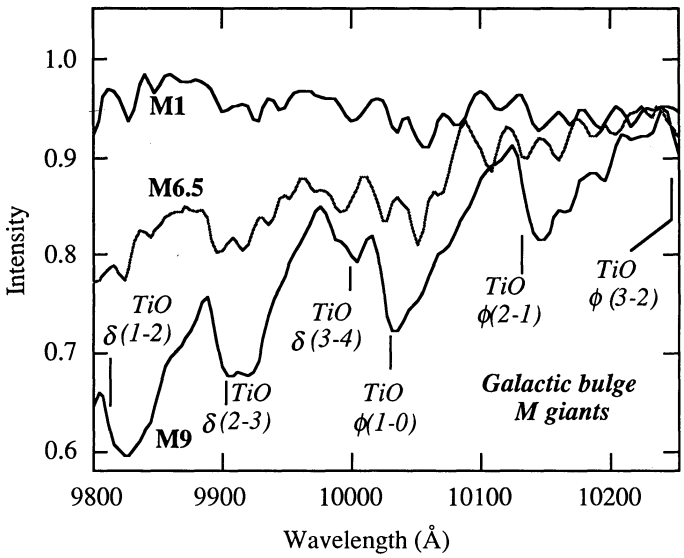

FIG. 3.—Spectral energy distribution of some galactic bulge M giants showing the steep change in continuum slope with spectral type and the location of the TiO band heads.

does not appear to be strong except for the later types in which the FeH molecule clearly dominates.

3. WING-FORD BAND MEASUREMENTS

The WFB feature was detected in all galaxies and confirms the first observations reported in Paper I. Because the velocity range of our data is ~ 1500 km s^{-1} and, in addition, galaxies were observed at different positions along the slit it is clear that the observed feature is real and not an artifact of residual instrumental effects or faulty sky subtraction. Spectra of galaxies, shifted to the rest frame, are displayed in Figure 4. The WFB is easily seen in all of them as the feature centered around

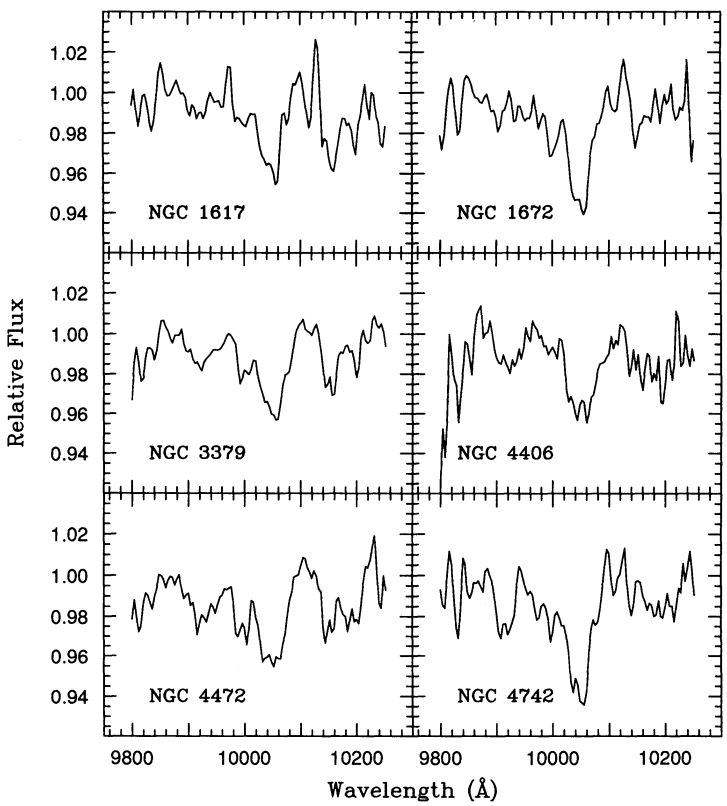

FIG. 4.—Continuum-normalized and background-subtracted spectra of each galaxy of the sample. The WFB feature is located around 9910 Å. The most prominent feature, located near 10050 Å, may be a superposition of FeH transitions and Paschen 7. S/N of each spectrum is better than 100 after sky subtraction. The vertical scale represents the relative flux normalized at 10100 Å.

9916 Å. In addition, the (3–4) band of the δ system of TiO with bandhead at 9986 Å is seen superposed on the wing of the strong absorption feature centered near 10050 Å. This indicates that the structure of the WFB in galaxies is determined not only by the FeH molecule but also by the (2–3) band of the same system of TiO, as seen in the spectra of giants. In galaxy spectra the feature near 10050 Å is probably dominated by Paschen 7 with contamination from the (1–0) band of ϕ system of TiO with bandhead at 10025 Å (Lockwood 1973), and by an additional FeH band. We discuss the latter in more detail farther on.

The strength of the WFB is given in Table 1 for the galaxies of our sample. The first four columns list respectively the identification of the galaxy, the de Vaucouleurs type, the radial velocity and the velocity dispersion of the central regions. Column (5) gives the WFB index as defined by the general expression

$$\Delta_1 = -2.5 \log [L/(C1^a \times C2^b)] ,$$

where L, C1, and C2 are the integrated flux (per Å) of the WFB feature and the two continua, respectively. The exponents in the above relation are defined as

$$a = \frac{\text{center}_{C2} - \text{center}_L}{\text{center}_{C2} - \text{center}_{C1}} ,$$

$$b = \frac{\text{center}_L - \text{center}_{C1}}{\text{center}_{C2} - \text{center}_{C1}} .$$

This definition becomes identical to the one used in Paper I and in Whitford (1977) for continuum-normalized symmetrical bandpasses. The quantities L, C1, and C2 have been defined in the same way as in Paper I and thus have been computed in 32 Å-wide bands, spaced by 50 Å, and centered, respectively, at rest-frame wavelengths of 9916, 9866, and 9966 Å. The index errors (col. [6]) have been estimated from Poisson statistics, and include errors from the sky subtraction as well.

The continuum band 2 (red side of the WFB) defined originally by Whitford (1977) is contaminated by the (3–4) band of the δ system of TiO. The behavior of the WFB index is thus dependent on the strength of that TiO band [in addition, the (2–3) band of the δ system of TiO is also contaminating the WFB feature as already mentioned in Paper I; a point we will discuss below]. In order to evaluate the effect of the choice of the continuum bands on the indices, we have redefined the continuum band 2. We give in column (7) of Table 1 the measure of the WFB index obtained after replacing the original continuum band by a 32 Å wide band centered instead at 10106 Å. Individual differences between the two series of values (cols. [5] and [7]) are small with a maximum of 0.007 mag (i.e., 2–3 σ), and an average difference of only 0.003 mag. In order to be consistent with previous studies, we have carried along both index definitions.

As shown in Table 1, with the exception of NGC 1672 the WFB has been clearly detected at better than the 3 σ level. Comparison with results from Paper I shows good agreement for the WFB measures of NGC 3379, NGC 4472, and NGC 4406 with differences of less than 1 σ for the two former galaxies and about 2 σ for the latter one. It should be stressed that the same observational setup has been used for the two observing runs. The consistency of results show the very high sensibility and stability of the CTIO Air Schmidt–CCD combination which are necessary in order to obtain the required S/N ratio and to subtract the contribution of the Meinel OH sky bands. We believe that this was the determining factor in explaining the failure to detect the feature in most previous studies (i.e., Whitford 1977; Carter, Visvanathan, & Pickles 1986). Cohen (1978), however, successfully measured the WFB for M31 and M32 and obtained respectively $\Delta_1 = 0.07 \pm 0.03$ and $\Delta_1 = 0.09 \pm 0.04$, values which are much larger than those obtained for the galaxies studied here.

In their recent investigation, Delisle & Hardy (1992) have measured the central arcsec of M31 and obtained $\Delta_1 = 0.036$ mag, thus confirming a fairly large value. Such a strong difference between these values and those of most other galaxies would require a very different mean stellar content. An alternative explanation could come from the very different physical areas involved in each sample (10–20 pc in Cohen's or in Delisle & Hardy's studies; ~ 1 kpc for the present more distant sample). If a dwarf enriched population lies in the nucleus of galaxies, or if the metallicity gradients are extremely steep near the very center, these effects could be measurable for the nearest galaxies while largely diluted for the more distant ones. Observations at much higher spatial resolution would be necessary to test these possibilities.

The WFB index average for the only two spirals in our sample is $\Delta_1 = 0.007 \pm 0.003$ from Table 1 while the average for ellipticals is $\Delta_1 = 0.016 \pm 0.003$. The difference between the two values is only significant at the 2 σ level, and may not be real. If it is, a possible interpretation would be that ellipticals are richer in low-mass stars than spirals, or that they differ significantly in metallicity.

The WFB of FeH has a weak dependency on metallicity. Mould & Wyckoff (1978) have shown that for M dwarfs, whose atmospheres are composed mainly of H_2, the following relation stands

$$n(\text{FeH})/n(\text{H}^-) \propto g^{1/2} Z^{1/4} ,$$

where g is the surface gravity and Z is the metal abundance. If we assume that ellipticals and spirals have the same stellar population (i.e., IMF, age) in their centers and that the band strength [i.e., the quantity $L/(C1^a \times C2^b)$] is proportional to the number of FeH molecules, the difference of the WFB index can be entirely accounted for if our sample shows the ratio $Z_{\text{Ell}}/Z_{\text{Sp}} \sim 1.4$ (or $\Delta[\text{Fe/H}] \sim 0.14$). This value is of the order of the precision usually obtained in determining galaxy metallicities. On the other hand, there is no correlation between total absolute magnitude and the WFB index for the ellipticals in our small sample. But the lack of correlation is not surprising if we consider the narrow range in total magnitude of our sample ($-19.5 \leq M_B \leq -22.5$) and the large scatter of the M_B–metallicity relation. In any case, interpretation of measured differences can only be undertaken through a large spectral interval comprising features sensitive to both the stellar mix and the metallicity.

The measurements of WFB indices for all stars, or combinations of stars, are presented in Table 2. We have divided the star sample in 28 groups according to their spectral types. Column (1) lists the identification of each group; column (2) gives their absolute magnitude in the I band. The procedure followed to compute these magnitudes will be described in § 5. The WFB indices Δ_1 and Δ_2 are given in columns (3) and (4), respectively.

It is known that in late M dwarfs the 9870–10070 Å spectral interval is dominated by a series of bands of the FeH molecule (Kirkpatrick et al. 1993; Phillips et al. 1987) of which the Wing-

TABLE 2

THE STELLAR LIBRARY

Groups (1)	M_I (2)	Δ_1 (mag) (3)	Δ_2 (mag) (4)	Δ_3 (mag) (5)	P7 (6)	Stars (7)
dF7	2.7	0.0026	0.0008	0.0145	0.0524	HR 2868
dF8	3.5	0.0026	−0.0019	0.0077	0.0427	HR 1536
dG8	5.1	0.0026	−0.0019	0.0016	0.0251	HR 3522
dK0	5.3	0.0053	0.0029	0.0059	0.0225	HR 2668
dK2	5.5	0.0052	0.0039	0.0067	0.0206	HR 1982
dK3	5.9	0.0060	0.0046	0.0045	0.0211	HR 1614
dK4	6.0	0.0137	0.0140	0.0079	0.0182	HR 5568
dM1	7.3	0.0489	0.0582	0.0237	0.0257	D 529
dM5	10.8	0.1128	0.1380	0.0547	0.0407	Barnard, Ross 128, Ross 614
dM6	11.7	0.2142	0.2652	0.1057	0.0690	Wolf 424
dM8	12.5	0.2761	0.3421	0.1361	0.0923	Wolf 359
sgF6	1.2	0.0056	−0.0009	0.0087	0.0469	HR 5323
sgK1	0.1	0.0073	0.0046	0.0054	0.0245	HR 1634
gK2	−0.2	0.0070	0.0064	0.0093	0.0291	HR 1509, HR 5854, HR 1953
gK3	−0.2	0.0087	0.0049	0.0058	0.0276	HR 5370
gM0.5	−1.6	0.0273	0.0311	0.0210	0.0365	HR 6056
gM1	−2.0	0.0136	0.0117	0.0070	0.0203	B 54
gM2	−2.4	0.0177	0.0111	0.0105	0.0125	B 78
gM3	−3.0	0.0163	0.0142	0.0108	0.0278	B 64
gM4	−3.7	0.0139	0.0168	0.0160	0.0280	B 96
gM5	−4.1	0.0359	0.0408	0.0307	0.0475	BMB 245
gM6.5	−4.6	0.0447	0.0466	0.0346	0.0338	BMB 235
gM8	−4.6	0.0538	0.0270	−0.0103	0.0476	BMB 87
gM9	−4.6	0.1064	0.0792	0.0185	0.0833	BMB 269, BMB 289
C1	−5.3	0.0360	0.0362	−0.0066	0.0122	ST 081, ST 140
C2	−5.6	0.0183	0.0173	0.0049	0.0043	ST 123, ST 142
S1	−4.6	0.1335	0.1593	0.0649	0.0744	S4A
S2	−4.6	0.1290	0.1333	0.0283	0.0485	S69A

Ford band is the strongest. It is very likely that the strong feature observed in Figure 2 near 10050 Å [hereafter denoted as $W(0–0)$] is composed of a series of transitions of the (0–0) system of FeH, three of which fall at 10050.4 Å (Phillips et al. 1987). This makes the interval chosen even more sensitive to the presence of late M dwarfs. Therefore we have introduced (col. [5]) a global FeH index covering the 9880–10070 Å interval which we denote as Δ_3 where L = 9880–10080 Å, C1 = 9840–9880 Å, and C2 = 10080–10120 Å.

The trend of $W(0–0)$ with spectral type for our stellar library is seen in Table 2 (col. [5]). Finally, we list in column (6) the values for the feature centered near 10050 Å and marked as P7. This feature, as discussed above, must also contain $W(0–0)$ which represents the only contribution to the feature for late K and M dwarfs. For this index we used the same definition as for the WFB index and with the same continuum C1, but with the band L now centered at 10058 Å and with a width of 64 Å, and the continuum band C2 centered at 10106 Å with a width of 32 Å. The trend with spectral type for the four indices is shown in Figure 5. The last column of Table 2 contains the name of individual stars composing each group. Star identifications preceded by B, BMB, ST, and S come from Blanco (1986), Blanco, McCarthy, & Blanco (1984) and Stephenson (1973), respectively. For spectral groups including more than one star, the features have been measured on the combined spectrum.

In general, the indices for the different spectral types are in good agreement with those of Whitford (1977), Cohen (1978), and Carter et al. (1986). For example, we obtain for Wolf 359 (spectral type dM8) the value $\Delta_1 = 0.276$ while Whitford's and Cohen's values are, respectively, $\Delta_1 = 0.26$ and $\Delta_1 = 0.27$. As expected, Table 2 indicates that the WFB index (col. [3]) is almost nonexistent for early dwarfs and becomes very important for dwarfs later than M1.

For giants, the WFB index is weak but becomes rapidly important for spectral types later than M4, a well-known result readily explained by the dominant effect of the (2–3) band of the δ system of TiO at ~9899 Å, which is very pronounced in late giants. The presence of this band is clearly established in giants by the nonequivocal presence of the (1–2) band of the same TiO system at 9814 Å. On the other hand, the presence in giants of this band (which is sensitive to metallicity) implies that the WFB index represents an upper limit to the contribution of dwarfs to the integrated spectra of galaxies through the FeH molecule.

The last two lines in Table 2 show a strong WFB index for S stars. These stars have a peculiar chemical composition (O/C ~ 1) which favors a low opacity, and thus a higher surface pressure in their atmosphere, leading to a higher FeH column density (Mould & Wyckoff 1978 and Nordh, Lindgren, & Wing 1977). Therefore, FeH is important for these peculiar giant stars.

Since the values of the WFB index for our galaxy sample are in good agreement with those of Paper I, we necessarily reach the same conclusion: no coeval models computed by Whitford (1977, his Fig. 3) give an index as weak as those we measured. Whitford's models have some important limitations such as the use of near-solar metallicity stars to analyze metal-rich spectra and the introduction of giant branches (up to ~M8–9) for which absolute luminosities and luminosity functions are still uncertain. The extensive stellar observations presented

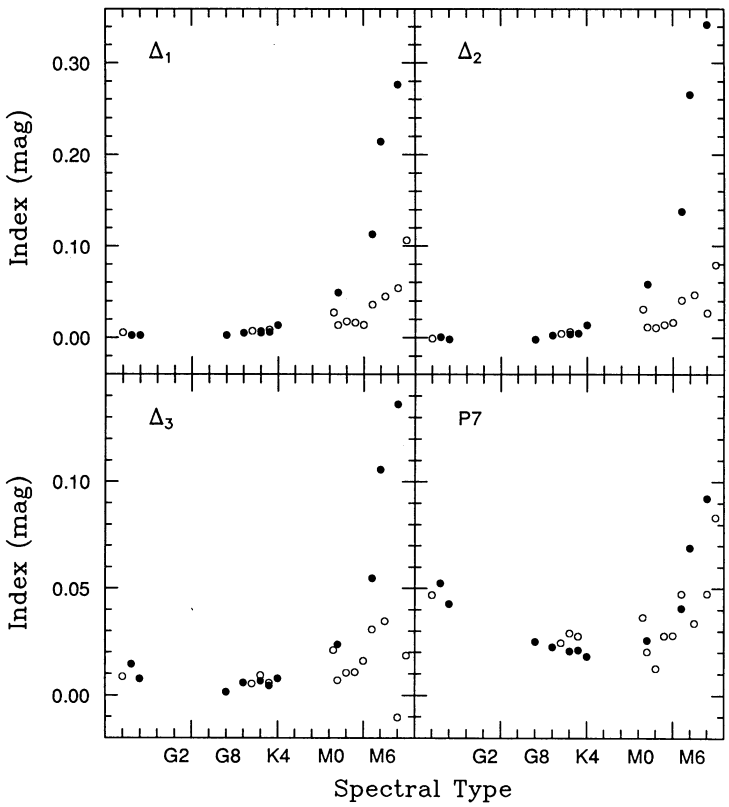

FIG. 5.—Trend with spectral type for all stars in the library of the four indices listed in Table 2. The filled and opened dots represent, respectively, the dwarfs and the giants of the library. C and S stars have been excluded and the subgiants have been grouped with the giants. For any of the three Δ indices, dwarfs, and giants later than M0 are well separated.

here together with improved synthesis methods will allow us to reanalyze the whole problem. The next two sections will be entirely dedicated to this aim.

4. OPTIMIZATION POPULATION SYNTHESIS

4.1. *Method*

The procedure used (Couture & Hardy 1990) consists in matching the observed spectrum $\boldsymbol{g}$ containing n spectral elements with a library L of m stellar groups which spectra also contain n spectral elements

$$\begin{pmatrix} l_{11} & l_{12} & \cdots & l_{1m} \\ l_{21} & l_{22} & \cdots & l_{2m} \\ l_{31} & l_{32} & \cdots & l_{3m} \\ \vdots & \vdots & \ddots & \vdots \\ l_{n1} & l_{n2} & \cdots & l_{nm} \end{pmatrix} \times \begin{pmatrix} x_1 \\ x_2 \\ \vdots \\ x_m \end{pmatrix} = \begin{pmatrix} g_1 \\ g_2 \\ g_3 \\ \vdots \\ g_n \end{pmatrix} .$$

The relative light contribution of the m stellar groups, designated above by the vector $\boldsymbol{x}$, is found by an optimization algorithm which minimizes the norm of the residual vector $\boldsymbol{r}$ defined as

$$\boldsymbol{r} = L\boldsymbol{x} - \boldsymbol{g} .$$

Physical constraints can be imposed in order to force the solution to comply with physically reasonable contributions from some given stellar groups. The simplest constraint of course is not to have any negative light contribution from any stellar group. We could also require that a subset of stellar groups obey a specific luminosity or mass function. For example, we could force the dwarf groups to follow a Salpeter law. All this can be done using the appropriate set of constraints; the algorithm still have to minimize the norm of the residual vector, as stated above, but now subject to constraints of the form

$$C\boldsymbol{x} > \boldsymbol{k} .$$

The matrix $\boldsymbol{C}$ has dimension $p \times m$, where p is the number of constraints. The constraints are defined by setting the elements of $\boldsymbol{C}$ and $\boldsymbol{k}$ to the appropriate values. For example, the non-negativity condition implies equating the matrix $\boldsymbol{C}$ with the identity matrix and setting all the elements of $\boldsymbol{k}$ to zero.

The n elements of the spectra do not have necessarily the same importance. Noise and sky emission or absorption lines or bands can make some portions of the spectra less reliable or simply useless. On the other hand, we may wish to increase the quality of the fit (e.g., decrease the residual vector as defined above) for some other portions of the spectra containing strong features. This can be accomplished by using a weight function containing n elements. The value of most elements is 1 while a smaller value (down to 0) is given to the elements corresponding to the less reliable wavelengths and a larger value (up to ~ 10) is given to the elements corresponding to the most significant wavelengths. This function is then multiplied into both the galaxy and the stellar library spectra.

4.2. *Results*

A stellar library, a set of constraints and a weight function have been defined as follows. The stellar library was built by ordering the observed stellar spectra in 28 groups as shown in Table 2. The whole available spectral interval (9800–10252 Å)

has been included. We imposed non-negativity constraints. We defined the weight function in order to maximize the quality of the fit specifically in the WFB spectral interval. Its first two and last two elements were set to "0," since the wavelength calibration is not well determined at the edges of spectra. The elements in the 9864–9964 Å spectral range were set to "3" while the value of all the other elements were set to "1." Different functions have been tested, using different weights for the WFB interval (from 1.5 to 10). It was found that a weight higher than 3 produces a bad fit for the continuum without improving significantly the fit of the WFB spectral area.

The synthesis results are shown in Table 3. The first column lists the stellar groups. Columns (2) to (7) give the relative light contribution (in percent) of each group within the observed bandpass (i.e., 9800–10252 Å) for each galaxy. The rms value of the fit is given at the bottom. In the absence of systematic effects, this value should correspond approximately to the mean noise of one spectral element. Some main trends are apparent. We do not see any contribution from M dwarfs later than M1, except for NGC 4742. This result is in good agreement with that of Zhou, Véron-Cetty, & Véron (1989). Giants, on the other hand, contribute about half of the light in the observed bandpass, most of it coming from M giants. The spectral interval used is not ideally suited to discriminate between K dwarfs and K giants. This could explain why the K dwarf contribution is so large. C and S stars contribute significantly (more than 2%) only for NGC 4406. This generally small contribution from S stars is fortunate since these stars possess also the FeH feature and could have been a source of ambiguity. It is for ellipticals that the later spectral types are present in the main sequence. This trend is in agreement with their stronger WFB measures, as already discussed. A strong contribution of F7 dwarfs has been obtained for NGC 4742. One of the main differences between the NGC 4742 observed spectrum and the spectra of other galaxies is the deeper feature located near the P7 position. If in galaxies the feature is indeed dominated by P7, this could suggest a younger population for NGC 4742, in agreement with the present synthesis results.

Synthesized spectra have been built by adding the different stellar spectra of the library according to their contribution as listed in Table 3. Figure 6 shows a comparison between the observed and synthesized spectra of NGC 3379, NGC 4406, and NGC 4742. The agreement is within 1% at any wavelength if we exclude the 50 Å intervals at the beginning and at the end of each spectrum. Tests were performed by excluding these intervals and no significant change in the relative contributions of stellar groups was detected. The last two lines of Table 3 contain the WFB measurements in the synthesized spectra using the first two index definitions. The Δ_1 values are all systematically larger than the measured strength of the original spectra by about 3 σ. However, the discrepancy between the two sets of Δ_2 values is marginal ($\sim 1.5\ \sigma$). While Figure 6 shows that the fit in the WFB region is good, the overall continua do show some systematic discrepancies, specially in the area of the "red" continuum used for the computation of Δ_1 (9950–9982 Å). This explains the disagreement we obtain when comparing Δ_1.

Systematic differences between the galaxies and the synthesized spectra could be explained by metallicity differences between stars included in the library and those composing the

TABLE 3

SYNTHESIS RESULTS FOR SIX GALAXIES

Groups (1)	N1617 (2)	N1672 (3)	N3379 (4)	N4406 (5)	N4472 (6)	N4742 (7)
dF7	...	8.4	...	5.5	1.6	26.0
dF8	...	...	...	...	...	...
dG8	...	...	...	...	...	...
dK0	42.1	35.9	50.7	13.1	8.0	...
dK2	...	...	...	16.8	...	...
dK3	...	...	...	...	...	...
dK4	15.6	...	4.8	...	56.0	...
dM1	...	...	1.1	12.6	1.7	12.5
dM5	...	...	...	...	...	4.7
dM6	...	...	...	...	...	...
dM8	...	...	...	...	...	...
sgF6	...	...	...	7.2	...	...
sgK1	...	...	...	...	...	5.2
gK2	6.8	16.1	...	...	...	...
gK3	...	...	...	...	...	...
gM0.5	...	...	14.8	...	7.1	...
gM1	...	...	...	...	...	15.9
gM2	...	...	...	...	...	...
gM3	7.5	7.0	0.7	...	...	...
gM4	1.3	7.0	3.5	17.7	...	18.4
gM5	9.9	4.6	3.4	2.2	1.2	...
gM6.5	6.1	12.9	9.8	7.7	16.6	6.7
gM8	8.7	8.1	11.2	7.7	7.8	8.5
gM9	...	...	...	...	...	...
C1	1.9	...	...	4.2	...	...
C2	...	...	...	5.3	...	...
S1	...	...	...	...	...	2.2
S2	...	...	...	...	...	...
rms (mag)	0.0100	0.0112	0.0075	0.0105	0.0104	0.0099
Δ_1 (mag)	0.018	0.017	0.020	0.021	0.023	0.027
Δ_2 (mag)	0.016	0.015	0.018	0.021	0.022	0.028

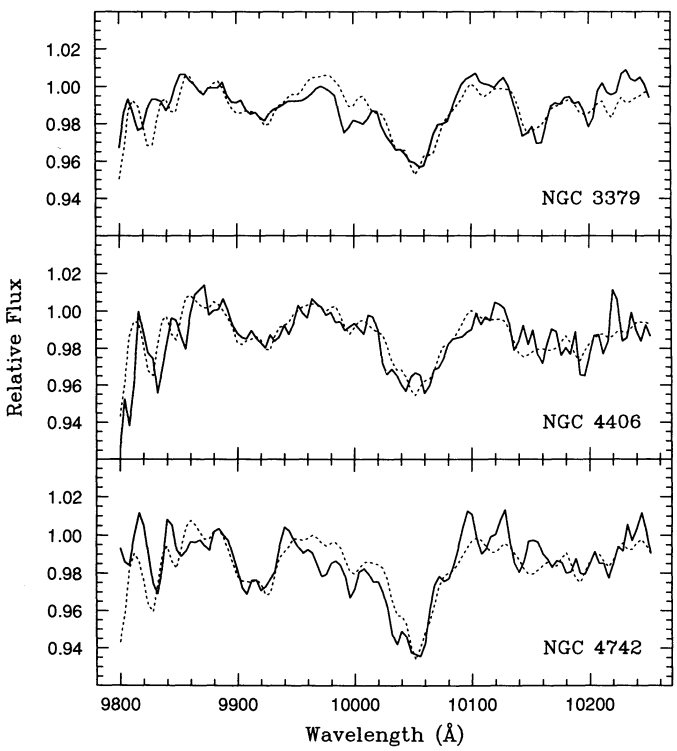

FIG. 6.—Spectra of three galaxies (*heavy lines*) superposed on the synthesized spectra (*dotted lines*) obtained from the best solution given by our optimization synthesis package. The fit is good at the 1% level over most of the spectral range.

galaxies. This is, of course, more important in the case of dwarfs for which the available metallicity range is small. Some incompleteness in the library could also mimic such an effect if the overall spectra of the missing stellar groups were very different from the spectrum of each stellar group in the library. We do not believe that residual effects due to the removal of sky emission bands could have caused these systematic differences.

We have done additional tests by synthesizing only a spectral interval of 112 Å around the WFB. We obtain a slightly better fit for the WFB but the wavelength interval redwards of 9970 Å (which was not used) was much bluer than before. The main change in the relative contribution of the stellar groups is the increase of the contribution of K dwarfs and giants at the expense of M giants. The contribution of M dwarfs has however remained approximately the same. The slight improvement in the quality of the fit in the restricted WFB spectral area does not compensate for the loss of astrophysical information caused by using only a restricted spectral interval of ~ 100 Å.

4.3. *Uniqueness*

The issue of uniqueness in dealing with stellar population synthesis is often regarded as one of the main uncertainties of the method; the other two being the usual incompleteness of the libraries used to fit the galaxy data, and the less than satisfactory knowledge of certain important phases of stellar evolution. In order to investigate the uniqueness of the synthesis solution, we have developed an algorithm which sweeps systematically the solution-space as follows. The first group in the library is selected and is assigned one of a number of prestablished contributions to the fit. An optimized solution is then obtained by allowing all other groups to vary freely. After the chosen group is cycled through all of the allowed fixed values of its contribution it is left variable and the next group is chosen for the same procedure. The operation is repeated until all groups present in the library have been allowed to participate in a similar way.

A series of optimized solutions are now available, each of them endowed with its associated probability in the form of a χ^2 value derived for that particular fit. A probability-weighted average of all solutions is then computed and a probability-weighted standard deviation is obtained for the contribution of each group. In our case the contribution of each of the 28 stellar groups was sequentially varied in the range 0% to 90% in 5% steps. The 532 (e.g., 28 × 19) solutions thus obtained were then averaged, and the results are shown in Table 4 for each galaxy. The various columns have the same definition as in Table 3 except that a standard deviation "σ" is provided for each group. Comparison with Table 3 shows that the contribution of the most important stellar groups has spilled over to the adjacent groups, as expected on physical grounds. But no strong contribution from new groups have appeared, leading to the conclusion that no significant secondary minima exist in the solution-space. Therefore, any difference between the results listed in Table 4 and the "true" fit should originate from Poissonian noise, perhaps some systematic effects linked to the data reduction procedure (including sky removal), and/or incompleteness in the stellar library. The procedure described above to study the solution space is akin to the one employed by Schmidt, Bica, & Alloin (1990).

An additional test has been performed by *fixing* the contri-

TABLE 4

RESULTS FROM THE UNIQUENESS TEST FOR SIX GALAXIES

Groups (1)	N1617 (2)	N1672 (3)	N3379 (4)	N4406 (5)	N4472 (6)	N4742 (7)
dF7	0.6 ± 0.2	8.6 ± 0.4	1.0 ± 0.5	3.9 ± 0.3	1.5 ± 0.2	20.9 ± 0.5
dF8	1.4 ± 0.5	2.6 ± 0.8	0.5 ± 0.1	1.1 ± 0.3	0.6 ± 0.2	1.4 ± 0.7
dG8	2.2 ± 0.9	0.7 ± 0.2	0.3 ± 0.1	2.6 ± 0.6	1.1 ± 0.5	0.6 ± 0.2
dK0	28.2 ± 1.1	23.4 ± 0.9	34.8 ± 1.0	8.6 ± 0.6	9.4 ± 0.8	2.4 ± 0.5
dK2	2.8 ± 0.7	1.8 ± 0.5	4.0 ± 0.9	9.7 ± 0.7	2.8 ± 0.8	1.4 ± 0.4
dK3	2.8 ± 0.6	1.9 ± 0.4	1.4 ± 0.4	2.3 ± 0.6	1.3 ± 0.4	0.8 ± 0.2
dK4	12.4 ± 0.9	4.3 ± 0.8	7.8 ± 0.8	2.5 ± 0.6	33.8 ± 1.4	1.4 ± 0.4
dM1	1.6 ± 0.2	0.7 ± 0.2	3.1 ± 0.3	10.6 ± 0.3	3.7 ± 0.3	8.1 ± 0.5
dM5	0.2 ± 0.1	0.2 ± 0.1	0.1 ± 0.1	0.2 ± 0.1	0.1 ± 0.1	4.4 ± 0.3
dM6	0.6 ± 0.5	0.1 ± 0.1	———	0.1 ± 0.1	———	0.2 ± 0.1
dM8	0.1 ± 0.1	0.3 ± 0.2	0.1 ± 0.1	0.2 ± 0.1	0.2 ± 0.1	1.0 ± 0.1
sgF6	0.6 ± 0.3	0.7 ± 0.2	0.2 ± 0.1	5.8 ± 0.3	0.4 ± 0.1	1.1 ± 0.3
sgK1	2.7 ± 0.7	2.1 ± 0.5	1.7 ± 0.5	2.4 ± 0.6	1.9 ± 0.5	3.9 ± 0.5
gK2	7.1 ± 0.8	10.6 ± 0.9	4.0 ± 0.7	3.1 ± 0.7	3.2 ± 0.6	2.2 ± 0.6
gK3	1.2 ± 0.3	0.9 ± 0.2	0.6 ± 0.2	2.1 ± 0.5	0.8 ± 0.2	0.8 ± 0.2
gM0.5	2.5 ± 0.6	3.4 ± 0.8	7.3 ± 0.7	1.5 ± 0.3	6.4 ± 0.8	2.7 ± 0.7
gM1	1.6 ± 0.4	2.0 ± 0.5	1.2 ± 0.4	1.7 ± 0.4	1.4 ± 0.4	13.6 ± 0.7
gM2	0.7 ± 0.3	1.4 ± 0.9	0.5 ± 0.1	1.1 ± 0.7	0.5 ± 0.2	0.3 ± 0.1
gM3	4.5 ± 0.4	4.2 ± 0.4	2.8 ± 0.5	1.5 ± 0.4	2.3 ± 0.5	1.3 ± 0.3
gM4	2.8 ± 0.5	6.0 ± 0.6	3.4 ± 0.5	14.2 ± 0.6	2.8 ± 0.7	13.7 ± 0.8
gM5	7.2 ± 0.5	4.6 ± 0.6	4.8 ± 0.4	2.3 ± 0.2	2.8 ± 0.5	1.5 ± 0.4
gM6.5	6.0 ± 0.3	11.0 ± 0.4	9.4 ± 0.3	7.9 ± 0.2	15.1 ± 0.7	6.3 ± 0.3
gM8	8.3 ± 0.2	8.1 ± 0.2	10.0 ± 0.1	6.7 ± 0.1	6.9 ± 0.2	8.4 ± 0.1
gM9	0.1 ± 0.1	———	———	0.2 ± 0.1	0.1 ± 0.1	0.1 ± 0.1
C1	1.2 ± 0.1	0.3 ± 0.2	———	3.2 ± 0.1	0.2 ± 0.1	0.1 ± 0.1
C2	0.6 ± 0.2	0.1 ± 0.1	0.9 ± 0.8	4.3 ± 0.2	0.4 ± 0.2	0.1 ± 0.1
S1	0.1 ± 0.1	0.1 ± 0.1	0.1 ± 0.1	0.1 ± 0.1	0.1 ± 0.1	1.7 ± 0.1
S2	———	———	———	0.1 ± 0.1	———	———

TABLE 5

SYNTHESIS RESULTS WITH CONSTRAINTS ON M DWARFS

Groups	Const.	NGC 1617		NGC 1672		NGC 3379		NGC 4406		NGC 4472		NGC 4742	
	(%)	P	Δ_1	P	Δ_1	P	Δ_1	P	Δ_1	P	Δ_1	P	Δ_1
(1)	(2)	(3)		(4)		(5)		(6)		(7)		(8)	
dM1	0.0	36	0.018	26	0.017	27	0.020	29	0.020	29	0.022	26	0.027
dM1	2.5	36	0.018	26	0.017	26	0.020	30	0.020	28	0.023	26	0.027
dM1	5.0	35	0.018	26	0.018	26	0.020	31	0.020	28	0.023	26	0.027
dM1	10.0	33	0.018	26	0.018	23	0.020	30	0.020	27	0.023	26	0.027
dM1	15.0	31	0.020	26	0.021	20	0.022	30	0.022	25	0.025	26	0.027
dM1	20.0	29	0.022	25	0.023	18	0.024	27	0.023	23	0.026	26	0.027
dM5	0.0	36	0.018	26	0.017	27	0.020	30	0.021	28	0.023	27	0.027
dM5	2.5	34	0.018	25	0.018	24	0.020	28	0.022	26	0.023	26	0.027
dM5	5.0	30	0.019	24	0.019	20	0.021	26	0.022	24	0.024	26	0.027
dM5	10.0	25	0.020	20	0.021	11	0.021	18	0.022	18	0.025	25	0.027
dM5	15.0	21	0.026	11	0.026	6	0.028	11	0.027	11	0.029	23	0.028
dM5	20.0	13	0.032	7	0.032	2	0.033	5	0.032	7	0.033	19	0.034
dM6	0.0	36	0.018	26	0.017	27	0.020	30	0.021	28	0.023	26	0.027
dM6	2.5	31	0.019	26	0.019	21	0.021	25	0.022	24	0.024	27	0.027
dM6	5.0	26	0.021	23	0.022	13	0.023	17	0.022	18	0.026	27	0.027
dM6	10.0	14	0.030	9	0.031	3	0.032	5	0.031	7	0.032	23	0.032
dM6	15.0	3	0.037	3	0.038	0	0.039	1	0.038	2	0.039	13	0.040
dM6	20.0	0	0.049	0	0.049	0	0.050	0	0.049	0	0.050	1	0.050
dM8	0.0	36	0.018	26	0.017	27	0.020	30	0.021	28	0.023	26	0.027
dM8	2.5	30	0.019	27	0.020	20	0.021	24	0.022	24	0.025	28	0.027
dM8	5.0	24	0.022	19	0.023	12	0.024	13	0.024	17	0.027	29	0.027
dM8	10.0	7	0.035	6	0.035	1	0.036	2	0.036	4	0.037	19	0.037
dM8	15.0	0	0.045	1	0.045	0	0.045	0	0.045	0	0.045	2	0.046
dM8	20.0	0	0.059	0	0.059	0	0.060	0	0.059	0	0.060	0	0.060

bution of M dwarfs from 0% to 20% in steps of 2%. The results are shown in Table 5. The first two columns give respectively the group and the relative contribution used as a constraint in each iteration. Columns (3) to (14) give, for each galaxy, the probability that each solution is the exact one, and the WFB values for the synthesized spectrum. The WFB indices are approximately constant except when the contribution of dwarfs is forced to be large. Therefore, it seems that an optimization of the whole spectrum using simple constraints do not lead to low values of the WFB index. The largest probabilities generally occur when the contribution of each group is closer to that found in Table 3. Differences like those found for NGC 4742 with constraints on dM8 [where $P(5\%)$ is slightly larger than $P(0\%)$] are caused by the fact that the best solution was obtained from an optimization using the spectra multiplied by the weight function described above while the rms value is simply computed from the difference between the original and the synthesized spectra which is independent of any such function. As a rule of thumb, a probability of $\sim 50\%$ is usually obtained when the rms value is about equal to the mean noise, while a solution is considered acceptable when its probability is higher than $\sim 25\%$. Table 5 shows that the M1 dwarf group is not severely constrained up to a contribution of 20%. The dM5, dM6, and dM8 groups are however more severely constrained, providing a contribution not larger than about 10% for the former group and 5% for latter ones. These values are a bit larger for NGC 4742. These upper limits for the light contribution of M dwarfs may be unrealistically high since the relative contribution of M dwarfs and other stellar groups must be coupled via a luminosity or mass function. The use of stellar population models is therefore inescapable.

5. STELLAR POPULATION MODELS AND HYBRID POPULATION SYNTHESIS (HPS)

5.1. *Overview*

The use of optimization synthesis has been useful to set rough limits to the contribution of stars of different spectral types to the composite light of galaxies. However, physical information such as ages and mass functions cannot be directly obtained without using more sophisticated constraints. A simple way to obtain this information is to compare our data to a series of theoretical stellar populations built from a set of known physical parameters. We first discuss the parameters used in the models and define which parameters are relevant to the present study.

An object as complex as a galaxy is probably composed of more than one stellar population for which star-formation rate and spatial distribution within the host galaxy will have to be taken in account. In addition, each stellar population is usually characterized by its metallicity, its helium content, its age, and its IMF. The IMF is in turn characterized by one or more parameters describing its form (e.g., the slope "x" for a power law) and usually requires a lower and a higher mass cutoff. Differences in the evolution of these populations as well as different specific abundance ratios as [C, N, O/H] or [C, N, O/Fe] may eventually have to be taken into account. Our restricted spectral interval is obviously not equally sensitive to all these parameters. The weak sensitivity of the WFB to abundance should permit to remove metallicity as a free parameter. In building our library, we tried to observe stars as metal-rich as possible. We roughly estimate the average metallicity of the library as [Fe/H] $\sim +0.2$ which is probably

slightly smaller than in the galaxy centers observed for our sample ([Fe/H] $\sim +0.3/+0.4$). We have then considered a metallicity of [Fe/H] $\sim +0.3$ (or $Z = 0.04$) in our models. Since our wavelength interval is small, the helium content of the stellar population has only a small effect on the continuum of our spectra (as it was also the case for the metallicity) and we have considered a fixed value of $Y = 0.25$, an average value in most theoretical models. Age may have a more noticeable effect on the spectra. Even though we expect old populations to dominate, it is not impossible that star formation has taken place until a few Gyr ago (see O'Connell 1986 for a review). For simplicity, we will consider three categories of population ages: old (about 10 to 15 Gyr), intermediate (5 to 8 Gyr) and young (~ 3 Gyr). In addition, we will suppose star formation in starbursts of negligible duration compared to the age of the galaxies.

We expect the present data to provide information on the ratio of M dwarfs (via the WFB and other spectral features) to M giants (mainly via the continuum). When translated into the IMF, this information tells us roughly the proportion of M dwarfs compared to turnoff stars, because the latter are the progenitors of the late giants observed. That means that we are mainly sensitive to stars of about 1 $M_\odot$ and those of a few tenths of solar mass, and much less sensitive to stars of intermediate masses. Consequently, we do not expect to have much information on the precise shape of the IMF. We will therefore use a single power law in which the slope and the lower mass cutoff (hereafter $m_{\rm low}$) will be the relevant free parameters. The use of such a simple model is dictated by simplicity. Others could have been used including a low mass turnover, or a different power-law slope for low masses. But the expected lack of sensitivity to shape does not justify the added complexity. Our $m_{\rm low}$ parameter represents a point beyond which the M-dwarf light contribution in the 1 μm region is undetectable, and thus could be interpreted as a true cutoff, or as a turnover, or as a drastic slope change. This, of course, precludes any strong constraint on total mass.

The evolutionary paths of late M giants up to M9 are not well-known and this problem will be discussed in more detail below. Models including particular abundance ratios are usually not available for metal-rich populations (as an example, see the oxygen-enhanced isochrones of Bergbusch & Vandenberg 1991) and we will use the standard abundances of the Revised Yale Isochrones (Green, Demarque, & King 1987). In conclusion, the free parameters will be the age, the slope of the IMF (up to about 1 $M_\odot$) and the lower mass cutoff.

5.2. *Construction of Stellar Populations*

We need to build a set of stellar populations by combining the spectra of the different stellar groups present in our spectral library (see Table 2) according to some specific models. These models must contain procedures to distribute the stars as a function of mass (e.g., a mass function) and then to convert this function into a luminosity function (e.g., a mass/luminosity function is required). We first established a set of mass/luminosity functions according to the metallicity (Z), the helium content (Y) and the age of the populations we want to create. The tabular form of the Revised Yale Isochrones (Green et al. 1987) were used for this purpose. These tables contain, for every set of Z, Y, and age, a list of about 200 ficticious stars ordered by mass and for which characteristics such as their temperature, their colors in $U-B$, $B-V$, $V-R$, and $V-I$ and their absolute magnitude in the V band are displayed. The tables cover the main sequence from ~ 0.6 $M_\odot$ and the red giant branch for ages older than ~ 2 Gyr. None of the isochrones continues past the tip of the giant branch. We first interpolated linearly the tables for [$Z = 0.04$, $Y = 0.2$] and [$Z = 0.04$, $Y = 0.3$] in order to create a new set of tables valid for [$Z = 0.04$ and $Y = 0.25$] (the choice of these values has been discussed in the previous section). Next, we just had to select individual tables according to age, in which the mass/luminosity function is explicitly contained.

The mass function was generated via a program kindly provided to us, together with the isochrones, by the Astronomical Data Center at the NASA Goddard Space Flight Center. This program uses a power law and offers the possibility of choosing any exponent. The program also requires the subdivision of the whole magnitude interval of the population (from ~ 0.6 $M_\odot$ to the tip of the giant branch) in several bins. The use of magnitude bins instead of mass bins allows a more regular sweeping of the H-R diagram because of the way in which mass is mapped into magnitude. We finally produced, for each previously selected table, a new one (hereafter MF-table) containing the mass and the absolute luminosity in the I band (hereafter M_I) corresponding to the center of the bins, and the number of stars (hereafter $n_{\rm st}$) contained in each bin. It remains now the difficult task of making a correspondence between the stellar groups defined in Table 2 and the bins defined in the MF-tables. For practical reasons, we subdivided our 28 stellar groups in five categories: FGK dwarfs, M dwarfs, FGK giants, M giants, and C-S stars since they have to be analyzed separately.

Most of F, G, and K dwarfs of our sample have been studied extensively. Colors are usually known and temperatures have been generally obtained via atmospheric models. Since these stars do not have the same age, helium content and metallicity as defined in a given isochrone table, their colors, temperatures and absolute magnitudes do not fall on a single line. A fit over all the characteristics has been made for each star in order to associate the "best" single line in the isochrone table. For any population older than 3 Gyr, there is no star on the main sequence as massive as a dF8 star and $n_{\rm st}$ of both dF7 and dF8 groups have been set to 0. The existing isochrone tables do not contain masses lower than ~ 0.6 $M_\odot$. We thus have to use a different approach to supply the required characteristics for M dwarf groups. We first used colors, $T_{\rm eff}$ and $M_{\rm Bol}$ (see Liebert & Probst 1987 and Berriman & Reid 1987) of individual M dwarfs in our library to derive M_I. We then used the relation $\log(\text{mass}) = -0.176 M_{\rm Bol} + 1.119$ (Liebert & Probst 1987), valid for a mass lower than 0.4 $M_\odot$, to obtain the mass associated to each group. Finally, we extrapolated the different mass functions explicitly displayed in the MF-tables to obtain $n_{\rm st}$.

Stars included in the subgiants, GK giants and M0.5 giants groups are bright and have been well studied. Therefore the same procedure as for FGK dwarfs has been followed. We have also set $n_{\rm st} = 0$ for the sgF6 group for any population older than 3 Gyr. The M giants observed in this investigation are metal-rich stars located near the Galactic center through Baade's windows. We do not know the precise characteristics of these stars, particularly their metallicities which are in the 0.2–0.3 dex interval. For M1 III to M4 III groups, we used temperatures listed in table of Lee (1970) to interpolate the isochrone tables. Since the table of Lee (1970) is valid for solar metallicity, we assumed that the temperature for M1–M4 giant stars do not change with metallicity. The approximation should have a negligible effect on the deduced mass and there-

fore on n_{st} since the mass changes much more slowly than the temperature on the giant branch. The effect on the deduced M_I could however be important and will be tested below. The M5–M9 giants and the C and S stars are in an advanced stage of evolution which is not yet very well understood. Their general characteristics are ill-defined and in addition would require some sort of extrapolation of the isochrone tables. We decided to exclude these eight groups from the populations we are building and to consider them as extra free parameters when needed.

Each MF-table previously selected has been rebinned and expanded (to include M dwarfs) in order to produce one bin for each of the first 20 stellar groups listed in Table 2. The bin limits were arbitrarily defined as the average of the masses of two adjacent groups. The parameter m_{low} has been included in removing all groups (if any) having a high bin limit smaller than m_{low} and in truncating to m_{low} the adjacent group. The new n_{st} were computed in summing the old ones within the new bin limits. A mean M_I was also computed for each bin. This last value was weighted by the n_{st} distribution according to the specific mass function used. Finally, the spectrum of each group was multiplied by the new n_{st} and divided by a factor F_{total}/F_{mean} where F_{total} represents the integrated flux of the spectrum in our observed bandpass and F_{mean} represents the relative flux corresponding to the mean M_I. This factor gives the relative number of stars of each group necessary to produce the same flux at 10100 Å (e.g., the normalization we used). Doing so, we implicitly assumed that the ratio of the absolute flux in the I band from group to group is the same as the ratio of the absolute integrated flux (e.g., F_{total}) in our bandpass. This approximation is necessary since calibrated fluxes around 10000 Å are not available for most spectral types.

Figure 7 shows the effect of (*a*) age, (*b*) "x," and (*c*) m_{low} on population spectra. The three curves in Figure 7*a* represent a population of 15 Gyr (*continuous line*), 8 Gyr (*dotted line*), and 3 Gyr (*dashed line*) with "x" = 1.35 and $m_{low} = 0.08\ M_\odot$. As one would expect, the spectra become slightly bluer and show a deeper P7 feature when the age decreases, especially from 8 to 3 Gyr. Similar changes are obtained if we use other values of "x" and m_{low}. Notice that 3 Gyr is the youngest age in the Revised Yale Isochrones for which giant branch has been computed. In Figure 7*b*, the continuous, dotted, and dashed lines represent, respectively, a population with a MF slope of 0.0, 1.35, and 3.0 with an age of 15 Gyr and $m_{low} = 0.08\ M_\odot$. No important change occurs if we compare the spectra with "x" = 0.0 and "x" = 1.35. However, the spectral features, and in particular the WFB, become much deeper from "x" = 1.35 to "x" = 3.0. A similar trend is seen using a different age. The changes are however much less significant for $m_{low} = 0.4\ M_\odot$. In Figure 7*c*, the three curves represent populations having 15 Gyr, a MF slope of 3.0 and m_{low}-values of 0.08 $M_\odot$ (*continuous line*), 0.2 $M_\odot$ (*dotted line*), and 0.4 $M_\odot$ (*dashed line*), respectively. The WFB (and at some extent the other features) becomes deeper when m_{low} decreases. This trend is the same, independently of age, but smaller with a slope of 1.35 and 0.0. We conclude that age is the least sensitive parameter while the effect of "x" and m_{low} is quite similar in the spectral range studied here.

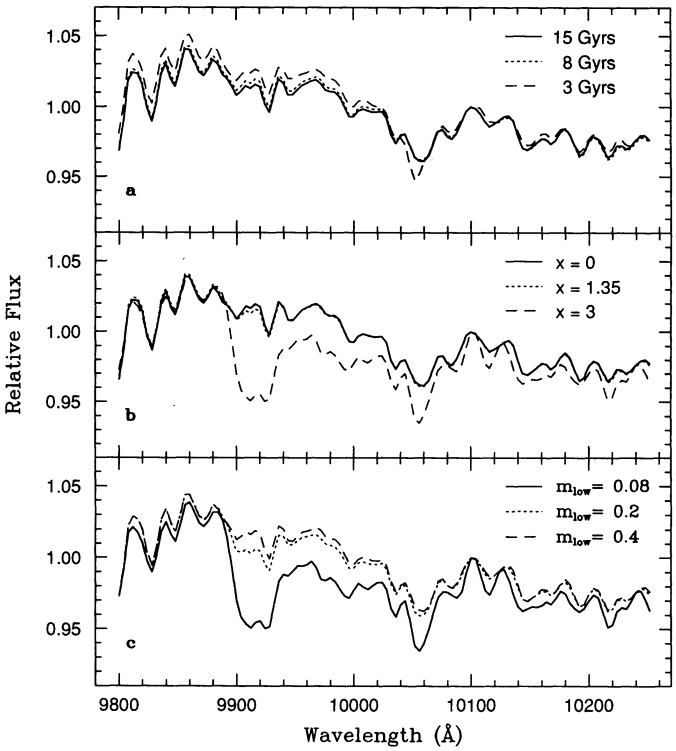

FIG. 7.—Stellar population models showing the effect of the three physical parameters we tested. The effect of age is shown in (*a*) where the three curves represent populations following a Salpeter law (e.g., "x" = 1.35, $m_{low} = 0.08\ M_\odot$) but having three different ages. The effect of "x" is shown in (*b*) where the three populations have an age of 15 Gyr and $m_{low} = 0.08\ M_\odot$. The effect of m_{low} is displayed in (*c*) where the three populations have an age of 15 Gyr and a MF slope "x" of 3.0.

5.3. *Calibration of the WFB Index*

We are now ready to calibrate the WFB index in terms of our parameters. We varied "x" and m_{low} only, given the weak sensitivity of the WFB to age. We built 132 different stellar populations with a fixed age of 15 Gyr and values of the slope "x" ranging from −1.0 to 4.0 in steps of 0.5, and m_{low} ranging from 0.1 to 0.6 $M_\odot$ in steps of 0.05 $M_\odot$. Populations with $m_{low} = 0.08\ M_\odot$ have also been considered. Our model populations are however unrealistic since they contain giants up to M4 only. We then added to each population the average contribution of M5–M9 giants taken from Table 3. Therefore each resulting population comprises 77.7% of the coeval populations to which contributions of 3.6%, 10%, and 8.7% for M5, M6.5, and M8 giants were added. Notice that no contribution for M9 giants has been added, in agreement with Table 3. We then measured the WFB index (Δ_1) for each population.

The results are shown in Figure 8*a*, where the WFB indices are displayed as "isoindices." The x-axis and y-axis represent respectively the slope "x" and the lower mass cutoff m_{low} of the mass function within ranges defined above. A horizontal line has been drawn at $m_{low} = 0.1\ M_\odot$ and allows a comparison with the unidimensional calibration of Whitford (1977; his Fig. 3). For any value of "x," the WFB index is systematically lower than those obtained by Whitford despite the fact that we used "metal-rich" library and isochrones rather than solar metallicity ones. This result is encouraging since all of Whitford's indices in his Figure 3 are significantly too high to agree with any WFB index measured in a galaxy with the exception (as previously discussed) of M31 and M32. Differences (see § 3), in chosen metallicities and isochrones, in absolute magnitudes of stellar groups and in the proportion of bright red giants could explain the discrepancy. We point out here that we used a more realistic library and that our assumptions on the contri-

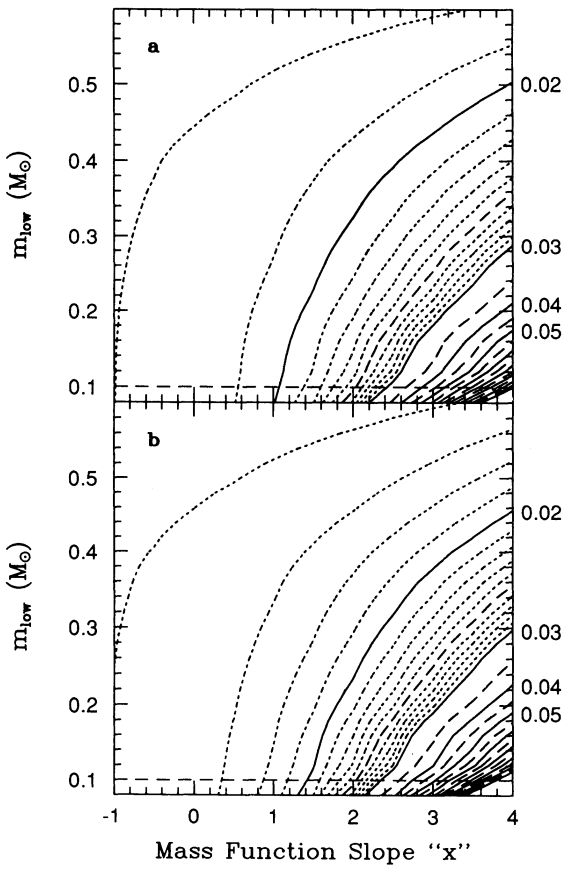

FIG. 8.—(*a*) Plot of Δ_1 isoindices from a set of populations of 15 Gyr and with "x" ranging from −1.0 to 4.0 (x-axis) and m_{low} ranging from 0.08 $M_\odot$ to 0.6 $M_\odot$ (y-axis). Numerical contributions of 3.6%, 10%, and 8.7% corresponding, respectively, to M5, M6.5 and M8 giants, as in Table 6, have been added to each population. The interval between two dotted contours is 0.001 mag while the interval between two continuous contours or two dashed contours is 0.01 mag. The values of continuous, dashed and dotted contours cover, respectively, the range 0.02–0.1, 0.025–0.095, and 0.018–0.029. (*b*) Same as previous panel but for the Δ_2 indices. The dotted contours now span the interval 0.016 to 0.029.

bution of red giants are looser. The WFB values shown in Figure 8 are not low enough to assign a "realistic" value of "x" and m_{low} for any of the galaxies of our sample (see Table 1). Thus, the same problem as in Whitford's models arises here for Δ_1, but to a lesser extent.

A straightforward cause of the systematic differences could be a bad estimate of absolute magnitudes (M_I) for some of the stellar groups composing the populations. As discussed above, the estimated M_I of M dwarfs and M giants are the most uncertain. We have redone the same computation as shown in panel (*a*) but after subtracting 0.5 magnitude from M_I of M dwarf groups. Even though the WFB values did decrease for each pair of ("x," m_{low}), the effect was not large enough to match the indices measured in galaxies. Changes from Figure 8*a* are even smaller if we alter the M_I values of the M0.5–M4 giant groups by 0.5 mag. Clearly, a faulty evaluation of M_I does not affect much the WFB index for a given population. We finally built an additional isoindex plot but using the Δ_2 definition. The results are shown in Figure 8*b*. Comparison with the values measured in ellipticals (see Table 1), shows that a Salpeter function ($x = 1.35$) with $m_{low} = 0.1$ or 0.08 is now possible. Figure 8 shows, not surprisingly, that the WFB index does not define a unique mass function. Clearly, a new method involving the *whole* observed spectral range must be employed. The next section is devoted to this aim.

5.4. *Hybrid Population Synthesis (HPS)*

We now attack the problem by combining in a common library two different categories of spectra: composite ones and individual stellar spectra for those stars which could not be included in the population models. In this "hybrid" approach we have thus replaced the stellar library we used in § 4.2 with a set of evolutionary populations built as in § 5.3, but without a contribution from the ill-understood evolutionary phases represented by the late M giants and the C and S stars. To this library of composite populations we have thus added the observed spectra of individual late giants not included in the evolutionary calculations. The advantage of using a library of stellar populations of known characteristics is that a fit to the observations provides insight into the physical properties (i.e., metallicity vs. age, star-formation rate, etc....) of the composite system. This is the rationale behind the method used by Bica & Alloin (1986a, 1986b) who derive their fiducial populations from the integrated spectra of star clusters of known ages and metallicities. In their case, however, the difficulty remains that the integrated spectrum of old and intermediate-age coeval metal-rich populations are so far largely unknown. Observations of metal rich stars are now possible and it is only because of the lack of understanding of the advanced phases of evolution leading, for example, to bright asymptotic-branch giants, that theoretical evolutionary models of old metal-rich populations seem still unreliable. This drawback is, of course, valid for any model which depends on these largely unknown phases of stellar evolution.

We have considered 27 composite populations with age of 15, 8, and 3 Gyr, "x" of 0.0, 1.35, and 3 and m_{low} of 0.08, 0.2, and 0.4 $M_\odot$. We recall that we used implicitly a metallicity of $Z = 0.04$ and a helium abundance of $Y = 0.25$. We thus have 35 different "spectral groups" in our new library. The same weight function as before has been used. The results are shown in Table 6 where column (1) gives the age/"x"/m_{low} of each population and the name of the independent stellar groups, column (2) gives the WFB index of each population and group, and columns (3) to (8) list the relative light contribution (in percent) within the observed bandpass 9800–10252 Å of each library component. The rms value of the fit and the WFB indices of the new synthesized spectra are given at the bottom of Table 6. Figure 9 shows a comparison between the observed (*heavy lines*) and the new synthesized spectra (*dotted lines*) for NGC 3379, NGC 4406, and NGC 4742.

We first notice that only a few (no more than three) populations are needed for each fit; which makes sense physically. The rms values are higher than the values obtained with the stellar library (see Table 3). This is not surprising since we expect the overall fit to deteriorate as we impose a set of specific mixtures instead of letting all stellar components adjust freely. On the other hand, the WFB indices themselves have almost the same value. A glance at Table 6 shows clearly that "x" = 3.0 and $m_{low} = 0.4\ M_\odot$ are to be preferred for four of the six galaxies of the sample. A high value of the MF slope is required to fit the continuum, whereas a large value of the lower mass cutoff prevents a deep WFB absorption feature to occur.

Since our spectral interval is not very sensitive to age, we tested the reality of a significant contribution from 3 Gyr population, as shown in Table 6, by forcing the solutions to

TABLE 6

HPS RESULTS FOR SIX GALAXIES

age/"x"/m_{low} (1)	Δ_1 (2)	N1617 (3)	N1672 (4)	N3379 (5)	N4406 (6)	N4472 (7)	N4742 (8)
15/0.00/0.08	0.011	...	...	...	...	...	...
15/0.00/0.20	0.011	...	...	...	...	...	...
15/0.00/0.40	0.010	...	8.6	...	...	...	...
15/1.35/0.08	0.014	...	...	...	...	...	...
15/1.35/0.20	0.013	...	...	...	...	...	...
15/1.35/0.40	0.011	24.3	...	...	...	...	...
15/3.00/0.08	0.059	...	...	...	...	...	...
15/3.00/0.20	0.023	...	...	...	...	...	...
15/3.00/0.40	0.014	60.5	...	58.2	13.4	75.8	...
8/0.00/0.08	0.010	...	...	...	...	...	...
8/0.00/0.20	0.010	...	...	...	...	...	...
8/0.00/0.40	0.010	...	...	...	...	...	...
8/1.35/0.08	0.013	...	...	...	...	...	...
8/1.35/0.20	0.012	...	...	...	...	...	...
8/1.35/0.40	0.010	...	...	...	...	...	...
8/3.00/0.08	0.056	...	...	...	...	...	...
8/3.00/0.20	0.022	...	...	...	...	...	...
8/3.00/0.40	0.013	...	...	...	...	...	...
3/0.00/0.08	0.010	...	...	...	...	...	...
3/0.00/0.20	0.010	...	...	...	...	...	...
3/0.00/0.40	0.010	...	71.9	...	...	...	...
3/1.35/0.08	0.012	...	...	...	...	...	...
3/1.35/0.20	0.011	...	...	...	...	...	...
3/1.35/0.40	0.010	...	...	...	...	...	...
3/3.00/0.08	0.059	...	...	...	...	1.8	...
3/3.00/0.20	0.023	...	...	...	15.0	...	79.6
3/3.00/0.40	0.013	0.1	...	22.1	44.8	...	...
gM5	0.036	...	...	...	3.1	...	...
gM6.5	0.045	9.5	13.9	12.3	8.8	18.0	11.0
gM8	0.054	5.7	5.6	7.5	5.5	4.3	8.6
gM9	0.106	...	...	...	...	...	...
C1	0.036	...	...	...	3.7	...	...
C2	0.018	...	...	...	5.8	...	...
S1	0.134	...	...	...	...	...	0.8
S2	0.129	...	...	...	...	...	...
rms (mag)	...	0.0105	0.0116	0.0084	0.0107	0.0110	0.0112
Δ_1 (mag)	...	0.018	0.017	0.020	0.021	0.022	0.029
Δ_2 (mag)	...	0.017	0.015	0.019	0.021	0.022	0.029

adopt an older age. It follows that use of only 15 Gyr populations provides fits almost indistinguishable from the optimal ones, except for NGC 4742. Accordingly, the detection of a younger population should be considered as doubtful, especially given the spectral interval used here.

NGC 1672 represents an exception to the main trend. The very mild WFB feature forced the solution to adopt a flatter slope or to use an even higher mass cutoff than those used in the fit. The young age we obtained was not reliable as we have just mentioned above. The other exception comes from NGC 4742 where the stronger absorption in the WFB has resulted in lower values of "x" and m_{low}. In this case the contribution from a 3 Gyr population cannot be effectively removed, in agreement with the strong contribution of F stars shown in Table 3. Therefore, it seems that NGC 4742 is indeed different from the other galaxies of the sample. Observations in a wider and bluer spectral range will be necessary to clarify the stellar content of this galaxy.

We have reapplied the HPS method by using populations with extreme values of "x" ("x" > 3.0) and m_{low} ($M_{low} > 0.4$ $M_\odot$). These populations have provided slightly better fits for NGC 1617, 3379, 4406, and 4472. This suggests that the slope and the lower mass cutoff of the stellar populations composing these galaxies could be even more extreme than those used in Table 6. However, the change in the rms value is less than 1% and these extreme populations do not seem significantly different from the preferred solution characterized by "x" = 3.0 and $m_{low} = 0.4$ $M_\odot$. We have also performed additional tests by forcing the solution to adopt a Salpeter law ("x" = 1.35 and $m_{low} = 0.08$ $M_\odot$). For the whole sample, the fit has worsened by 2%–5%. The Salpeter exponent is now located approximately on the same "isoindex" as the preferred solution (see Fig. 8). The use of the whole observed spectral interval has succeeded in narrowing the set of acceptable mass functions. The use of a larger interval, including the Na I doublet at 8183 and 8195 Å, and the Ca II triplet at 8498, 8542, and 8662 Å (see § 1), should eventually provide a better determination of the mass function.

A recurrent question in the literature has been that of the I light contribution of late dwarf stars to the integrated spectra of the central regions of galaxies. Although giant-dominated populations are generally recognized as being more likely (see Delisle & Hardy 1992 for a discussion and for references), the issue is far from settled (i.e., Boroson & Thompson 1991). We have attempted a solution by computing the percentage of the total luminosity which contributed by all dwarfs and by the M dwarfs alone for the 27 stellar populations displayed in Table 6. The results are shown in Table 7 in which the first column displays the three parameters characterizing the model (i.e., age/"x"/m_{low}). The remaining columns show the WFB indices,

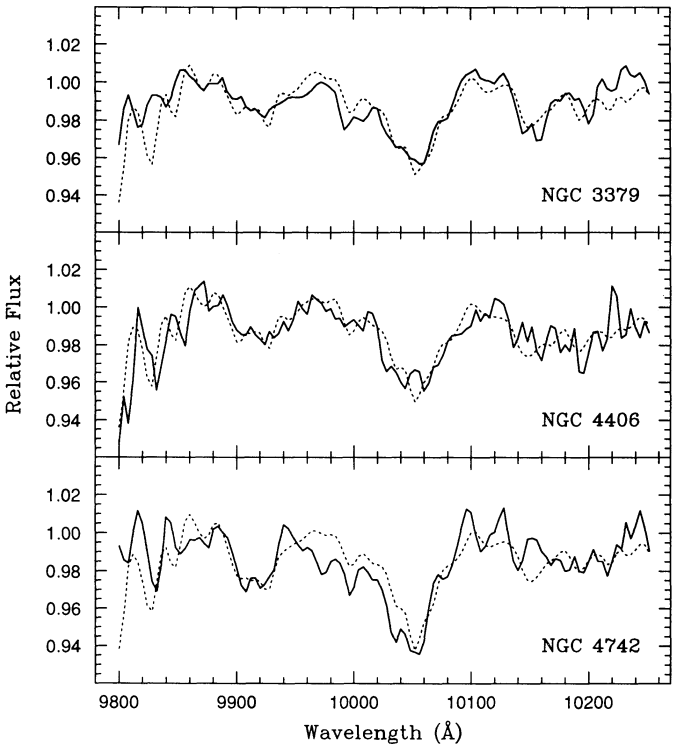

FIG. 9.—Spectra of three galaxies (*heavy lines*) superposed on the synthesized spectra (*dotted lines*) obtained from the best solution given by the Hybrid Population Synthesis method. The fit is good at the 1% level over most of the spectral range.

TABLE 7

CHARACTERISTICS OF POPULATIONS

age/"x"/m_{low} (1)	Δ_1 (2)	Δ_2 (3)	$\%_{Mdw}$ (4)	$\%_{dw}$ (5)
15/0.00/0.08	0.011	0.010	2.5	17.1
15/0.00/0.20	0.011	0.010	2.4	17.1
15/0.00/0.40	0.010	0.009	2.1	16.8
15/1.35/0.08	0.014	0.014	6.7	23.4
15/1.35/0.20	0.013	0.012	5.9	22.8
15/1.35/0.40	0.011	0.010	4.5	21.6
15/3.00/0.08	0.059	0.071	33.4	48.3
15/3.00/0.20	0.023	0.026	19.8	37.7
15/3.00/0.40	0.014	0.014	11.0	30.9
8/0.00/0.08	0.010	0.009	1.6	22.3
8/0.00/0.20	0.010	0.009	1.6	22.3
8/0.00/0.40	0.010	0.009	1.4	22.1
8/1.35/0.08	0.013	0.012	5.3	29.1
8/1.35/0.20	0.012	0.011	4.7	28.7
8/1.35/0.40	0.010	0.009	3.5	27.8
8/3.00/0.08	0.056	0.068	32.3	53.8
8/3.00/0.20	0.022	0.024	19.0	44.7
8/3.00/0.40	0.013	0.013	10.6	39.0
3/0.00/0.08	0.010	0.009	1.0	29.8
3/0.00/0.20	0.010	0.009	1.0	29.8
3/0.00/0.40	0.010	0.008	0.9	29.7
3/1.35/0.08	0.012	0.011	4.3	38.4
3/1.35/0.20	0.011	0.010	3.8	37.8
3/1.35/0.40	0.010	0.009	2.9	37.5
3/3.00/0.08	0.059	0.071	34.7	65.1
3/3.00/0.20	0.023	0.025	20.7	57.7
3/3.00/0.40	0.013	0.012	11.6	52.9

and the M dwarf and dwarf contribution in percentage units of *I* light. These models are probably unrealistic because of the lack of late giants but, precisely because of this, they should provide maximum contribution from late dwarfs as a result of the total lack of spectral compensation from late giants. We have presented in Figure 10 the dwarf contribution to the total luminosity in the form of isophotes drawn in the m_{low}–"x" plane. Panel (*a*) gives the contours of equal *I* luminosity produced only by M dwarfs, expressed as percentage of total *I* light. For this figure these contributions were computed through evolutionary synthesis using our stellar library and the same, i.e., 22.3%, fixed numerical contribution of M5–M9 giants as in Figure 7. Panel (*b*) of the same figure contains the same information but for all dwarfs. In general our results indicate that dwarfs rarely contribute as much as 50% of the *I* band luminosity, and usually less than 40%, whereas M dwarfs contribute less than 30% and usually less than 10%–20%. These results are generally compatible with those of Tables 3 and 4 obtained by optimization of the stellar library. The latter procedure however tends to suffer more from cross talk between K giants and dwarfs and this may explain the higher proportion of K dwarfs found there.

Finally, we have applied the HPS method by fixing a given combination of age/"x"/m_{low}, as indicated in the first column of Table 8, and allowing the M5–M9 giants to vary freely. The

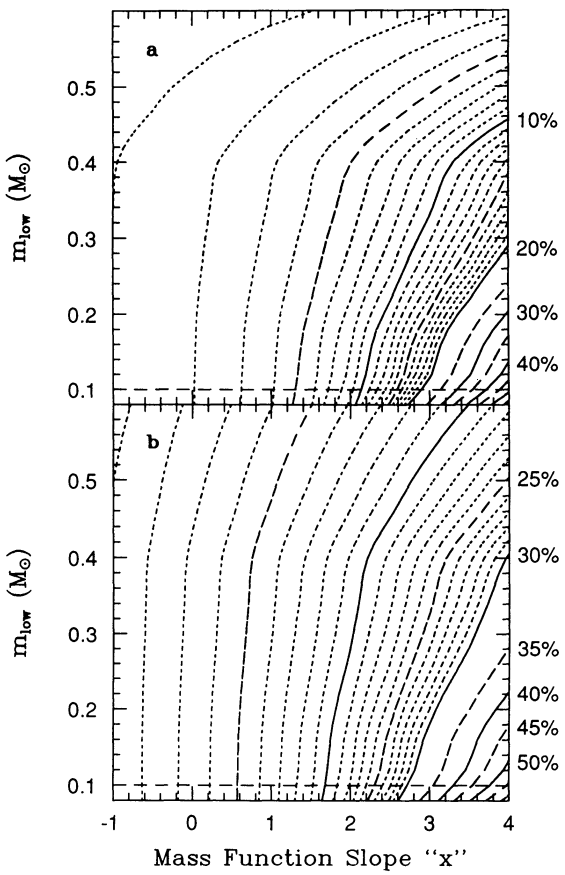

FIG. 10.—Dwarf contribution isophotes in the m_{low}–"x" plane. Panel (*a*) gives the contours of equal *I* luminosity produced by M dwarfs, expressed as percentage of total *I* light. These contributions were computed through evolutionary synthesis using our stellar library and the same, i.e., 22.3%, fixed numerical contribution of M5–M9 giants as in Fig. 8. Panel (*b*): same as (*a*) but for all dwarfs.

TABLE 8

LIGHT CONTRIBUTION OF DWARFS FROM HPS METHOD

age/"x"/m_{low} (1)	NGC 1617		NGC 1672		NGC 3379		NGC 4406		NGC 4472		NGC 4742	
	$\%_{M\,dw}$	$\%_{dw}$	$\%_{M\,dw}$	$\%_{dw}$	$\%_{M\,dw}$	$\%_{dw}$	$\%_{M\,dw}$	$\%_{dw}$	$\%_{M\,dw}$	$\%_{dw}$	$\%_{M\,dw}$	$\%_{dw}$
15/0.00/0.08	2.1	14.4	2.0	13.8	2.0	13.6	1.9	12.8	1.9	13.1	1.9	12.7
15/0.00/0.20	2.1	14.4	2.0	13.7	1.9	13.5	1.8	12.7	1.9	13.0	1.8	12.7
15/0.00/0.40	1.8	14.1	1.7	13.5	1.7	13.2	1.6	12.5	1.6	12.8	1.6	12.5
15/1.35/0.08	5.8	20.2	5.5	19.1	5.5	19.1	5.2	18.0	5.2	18.3	5.1	17.7
15/1.35/0.20	5.1	19.4	4.8	18.4	4.8	18.4	4.5	17.2	4.6	17.6	4.4	17.0
15/1.35/0.40	3.8	18.2	3.6	17.3	3.5	17.1	3.3	16.0	3.4	16.4	3.3	15.9
15/3.00/0.08	18.5	26.7	15.5	22.4	16.3	23.5	18.3	26.5	15.5	22.4	17.4	25.1
15/3.00/0.20	17.0	32.4	16.7	31.7	16.6	31.6	15.8	30.1	16.1	30.6	15.9	30.2
15/3.00/0.40	9.4	26.2	8.9	24.8	8.9	24.8	8.4	23.3	8.5	23.8	8.2	23.0
8/0.00/0.08	1.4	18.4	1.3	17.8	1.3	17.3	1.2	16.4	1.2	16.8	1.2	16.3
8/0.00/0.20	1.3	18.4	1.3	17.7	1.2	17.3	1.2	16.3	1.2	16.7	1.2	16.3
8/0.00/0.40	1.1	18.2	1.1	17.6	1.1	17.1	1.0	16.2	1.0	16.6	1.0	16.1
8/1.35/0.08	4.5	24.7	4.2	23.4	4.2	23.4	3.9	21.7	4.0	22.1	3.9	21.5
8/1.35/0.20	3.9	24.0	3.7	22.9	3.7	22.6	3.4	21.1	3.5	21.5	3.4	20.9
8/1.35/0.40	2.9	22.9	2.8	22.0	2.7	21.5	2.6	20.2	2.6	20.7	2.5	20.0
8/3.00/0.08	18.1	30.2	15.4	25.6	15.9	26.5	17.8	29.7	16.2	26.9	16.8	28.0
8/3.00/0.20	16.2	38.1	15.8	37.1	15.8	37.1	15.0	35.3	15.3	35.9	15.0	35.2
8/3.00/0.40	8.8	32.5	8.8	30.8	8.3	30.7	7.7	28.5	7.9	29.0	7.6	28.1
3/0.00/0.08	0.8	24.2	0.8	24.0	0.8	23.5	0.7	21.7	0.8	22.6	0.7	22.2
3/0.00/0.20	0.8	24.2	0.8	24.0	0.8	23.4	0.7	21.6	0.7	22.5	0.7	22.2
3/0.00/0.40	0.7	24.1	0.7	23.9	0.7	23.3	0.6	21.6	0.6	22.4	0.6	22.1
3/1.35/0.08	3.5	31.2	3.5	31.0	3.4	30.2	3.1	27.8	3.2	28.9	3.2	28.7
3/1.35/0.20	3.0	30.3	3.0	30.3	2.9	29.3	2.7	27.1	2.8	28.2	2.8	28.0
3/1.35/0.40	2.3	29.7	2.3	29.9	2.2	28.9	2.0	26.6	2.1	27.7	2.1	27.6
3/3.00/0.08	18.3	34.3	27.8	29.1	16.0	30.2	18.0	33.8	16.3	30.6	17.1	32.1
3/3.00/0.20	10.9	47.1	17.1	47.7	16.7	46.6	15.8	44.0	16.1	45.0	16.5	45.9
3/3.00/0.40	9.3	42.0	9.2	42.0	9.0	40.9	8.9	40.3	8.5	38.5	8.5	38.8
optimal	7.8	23.9	0.8	22.8	9.0	29.6	9.8	36.5	9.0	24.6	16.5	45.9

results are shown in the column corresponding to each galaxy. The outcome from the optimal solution of Table 6 is included in the last line of Table 8. The overall conclusion is that dwarfs contribute less than 30%–40% of the I light, and that M dwarfs contribute less than 10%–20%. These results are in good general agreement with those of Carter et al. (1986).

6. CONCLUSIONS

We summarize our findings:

1. The WFB has been measured for six galaxies, confirming and extending the results obtained in Paper I. Our results are qualitatively consistent with those of Whitford (1977) in that the WFB indices measured on galaxy spectra tend to be lower than those computed by the models, although in our case the disagreement was reduced.

2. We have used the whole observed spectral range (9800–10252 Å) in order to synthesize the galaxy spectra. This is fundamental because we want to introduce as much continuum information as possible and because the feature near 10050 Å may also contain a contribution from the FeH molecule. We have used a new near-IR metal-rich stellar library based on stellar observations of galactic bulge giants obtained during the same run. With the exception of NGC 4742, we do not detect a strong contribution of late M dwarfs. Most of the contribution comes from dwarfs earlier than M5, although lack of stars of types dM2 through dM4 in our library prevents a finer analysis.

3. We have used a new synthesis method (Hybrid Population Synthesis), which involves a combination of evolutionary models and individual stellar spectra, to obtain information on the main sequence mass function compatible with our galaxy data. No strong conclusion as of the structure of the MS luminosity function has been reached. In general, no age discrimination was possible, but a preferred mass function with a steep slope of "x" ~ 3 and a lower mass cutoff of $m_{low} \sim 0.4$ has been obtained. Thus, despite the *apparent* weakness of the WFB, the present study shows that a steep mass function slope cannot be ruled out, and may even be preferred, if an appropriate lower mass cutoff is employed. This study is insensitive to Rose's (1985) suggestion of the presence of a turn-off corresponding to an intermediate age population, given the insensitivity to age effects of our spectral range (see Table 6 and Fig. 7).

NGC 4742 would seem to be special in that a smaller slope "x" ~ 2.5 and a smaller cutoff $m_{low} \sim 0.1$ is likely, and a significant young component could be present in this specific case, although our solution only suggests but does not absolutely require a younger age. It would be interesting to confirm the presence of this young population through observations near 4000 Å, Rose's (1985) preferred spectral region, and thus test the sensitivity of P7 to age. At the other extreme, the WFB index of NGC 1672 is much lower than the other galaxies and the best fit using the HPS method requires a lower slope ("x" ~ 0.0) or/and a higher cutoff ($m_{low} > 0.4\ M_{\odot}$). The WFB original indices (i.e., Δ_1) as measured on the observed spectra are significantly lower than those measured on the synthesized spectra created from the fits. In fact, these original values can barely be accommodated in our "x"–m_{low} plane (see Table 3 and Fig. 8*a*) and should thus imply very extreme "x" and/or m_{low}-values (see Paper I). The picture changes somewhat when we use a new definition of the band (see Table 3 and Fig. 8*b*), namely Δ_2, which depends differently on the continuum-band definition. In any case, the good fit obtained for the WFB area (see Figs. 5 and 8) suggests that the right proportion of M

dwarfs may have been determined even though the two sets of WFB indices differ.

As expected, the HPS method as applied to the full spectral range available has been more successful in determining a narrower range of mass functions than the use of the WFB spectral index alone. Spectral studies of stellar populations in galaxies clearly require a global approach. The use of a few spectral features, while less consuming of telescope time and easier to analyze, often provides results of questionable reliability (see Delisle & Hardy 1992, and references therein). This is particularly true of the use of spectral indices, which are very often extremely sensitive to the way the continuum bandpasses are defined. It is clear that the complete set of parameters characterizing a stellar population can only be obtained if the analysis is performed simultaneous on the whole spectra, starting from at least as low in wavelength as 4000 Å where turnoff dwarfs may dominate the integrated light. Acquisition of high S/N spectra of galaxies over a wide spectral interval, improvements of stellar libraries and a better understanding of the late stellar evolution are then the unavoidable premises to any study capable of determining the MS mass function precisely.

4. Finally—and these are perhaps the strongest results of our investigation—it has been demonstrated by fitting the observations of galaxies via the HPS method (see Table 8) that no combination of model parameters is capable of producing a luminosity contribution in the *I* band coming from M dwarfs larger than about 20%. Also, the total luminosity contribution in the *I* band coming from *all* dwarfs would rarely exceed 40%. Populations with a Salpeter exponent of the mass function, which are not excluded, will contribute on average less than 5% of the light in the *I* band from M dwarfs and less than 20% from all dwarfs.

We are grateful to AURA and CTIO for the granting of observing time and for the, as usual, excellent support provided during the observations. We thank the Astronomical Data Center at the NASA Goddard Space Flight Center for providing the Revised Yale Isochrones. The referee, Andrew Pickles, is to be thanked for having made useful comments concerning mass function models. We gratefully acknowledge financial support through the Natural Sciences and Engineering Research Council of Canada, the National Research Council, and the Fonds FCAR du Québec.

REFERENCES

Bergbusch, P. A., & Vandenberg, D. A. 1991, preprint
Berriman, G., & Reid, N. 1987, MNRAS, 227, 315
Bica, E., & Alloin, D. 1986a, A&A, 162, 21
———. 1986b, A&AS, 66, 171
Blanco, V. M. 1986, AJ, 91, 290
Blanco, V. M., McCarthy, M. F., & Blanco, B. M. 1984, AJ, 89, 636
Boroson, T. A., & Thompson, I. B. 1991, AJ, 101, 111
Carter, D., Visvanathan, N., & Pickles, A. J. 1986, ApJ, 311, 637
Cohen, J. G. 1978, ApJ, 221, 788
Couture, J., & Hardy, E. 1990, AJ, 99, 540
Davidge, T. 1990a, AJ, 99, 561
———. 1990b, ApJ, 351, L37
Delisle, S., & Hardy, E. 1992, AJ, 103, 711
Faber, S. M., & French, H. B. 1980, ApJ, 235, 405
Green, E. M., Demarque, P., & King, C. R. 1987, Revised Yale Isochrones and Luminosity Functions (New Haven: Yale Univ. Obs.)
Hardy, E. 1990, in Proc. ESO/CTIO Workshop on Bulges of Galaxies, ed. H. E. Schwartz, & D. Terndrap (Garching: ESO), 209
Hardy, E., & Couture, J. 1988, ApJ, 325, L29 (Paper I)
Jones, J. E., Alloin, D. M., & Jones, B. J. T. 1984, ApJ, 283, 457
Kirkpatrick, J. D., Kelly, D. M., Rieke, G. H., Liebert, J., Allard, F., & Wehrse, R. 1993, ApJ, 402, 643
Lee, T. A. 1970, ApJ, 162, 217
Liebert, J., & Probst, R. G. 1987, ARA&A, 25, 473
Lockwood, G. W. 1973, ApJ, 180, 845
Mould, J. R., & Wyckoff, S. 1978, MNRAS, 182, 63
Nordh, L., Lindgren, B., & Wing, R. F. 1977, A&A, 56, 1
O'Connell, R. W. 1986, in Space Telescope Science Institute Symp. 1, Stellar Populations, ed. C. A. Norman, A. Rensini, & M. Tosi (Cambridge: Cambridge Univ. Press), 167
Phillips, J. G., Davis, S. P., Lindgren, B., & Balfour, W. J. 1987, ApJS, 65, 721
Rose, J. A. 1985, AJ, 90, 1927
Schmidt, A. A., Bica, E., & Alloin, D. 1990, MNRAS, 243, 620
Stephenson, C. B. 1973, Publ. Warner & Swasey Obs., 1, 4
Whitford, A. E. 1977, ApJ, 211, 527
Whitmore, B. C., McElroy, D. B., & Tonry, J. L. 1985, ApJS, 59, 1
Zhou, X., Véron-Cetty, M.-P., & Véron, P. 1989, A&A, 211, L12